

Monte Carlo simulation in Fermi systems: transport parameters

This article has been downloaded from IOPscience. Please scroll down to see the full text article.

1990 J. Phys.: Condens. Matter 2 4717

(<http://iopscience.iop.org/0953-8984/2/21/006>)

View [the table of contents for this issue](#), or go to the [journal homepage](#) for more

Download details:

IP Address: 171.66.16.103

The article was downloaded on 11/05/2010 at 05:56

Please note that [terms and conditions apply](#).

Monte Carlo simulation in Fermi systems: transport parameters

L Romanó and V Dallacasa

Dipartimento di Fisica dell'Università di Parma, Viale delle Scienze, 43100, Parma, Italy

Received 10 May 1989, in final form 6 March 1990

Abstract. A Monte Carlo technique for charge transport is applied to a Fermi system in which the electron–phonon scattering is described by means of perturbation theory and the Fermi statistics are achieved by the use of an appropriate algorithm. The stationarisation conditions of the system are studied, and it is found that the transport parameters obtained by the simulations as a function of temperature are in good agreement with the theory of metals. Possible extensions to the low-resistivity states are suggested.

1. Introduction

In recent years, Monte Carlo simulations have been used successfully for the study of the transport properties of semiconductor and insulator materials under conditions of high electric fields, and recently also for the description of microdevices [1–3]. On the contrary, in metals they have been scarcely used because the driving field causes only small deviations from thermal equilibrium and especially because the electrons follow the Fermi statistics, while the usual Monte Carlo model describes Boltzmann systems.

In a previous paper [4] we presented an application of an ensemble Monte Carlo simulation to a model of a metal using an appropriate algorithm, first applied by Lugli and Ferry [5] for the description of degenerate semiconductors, to take into account the Pauli exclusion principle. This was an early test of the applicability of the technique to simple metals for the study of electron–phonon interactions. In this work we present a development of the Monte Carlo technique applied to metallic systems to study the transport parameters and their behaviour as a function of the temperature. In particular, we study the resistivity versus temperature choosing as estimator the longitudinal diffusion coefficient and using the Einstein relation. We present some results which are in good agreement with the theory of metals at high and low temperatures indicating that it is possible to apply this technique to a normal state of the metal using a reasonable computer amount of time in order to treat the electron–phonon coupling and transport parameters. It is possible then to envisage the application of the same technique to realistic situations for metals in the normal state as may happen close to the transition to the superconductivity state.

2. The numerical simulation

The ensemble Monte Carlo simulation used in this paper is based on following the story of a sufficiently large number of electrons ($N = 10^5$) for a given time interval t_m

within a volume $V_c = N/n \simeq 10^{-17} \text{ cm}^3$, where $n = 10^{22} \text{ cm}^{-3}$ is the typical electronic concentration of a metal. A constant electrical field of the order of 1 V cm^{-1} is applied in the z direction. The electrons are injected at $t = 0$ into the crystal with an appropriate energy distribution $g(\epsilon, 0)$. Generally in our Monte Carlo simulations we use an initial distribution $g(\epsilon, 0)$ close to that expected at infinite time because we are interested in the study of the steady state of the system.

During the time t_m we make ~ 30 observations of the state of motion of each electron. For the sake of simplicity the observations are made at regular time intervals Δt ; at each Δt the following quantities are recorded:

$$\langle z \rangle \tag{1}$$

$$\langle x^2 + y^2 \rangle \tag{2}$$

$$\langle (z - \langle z \rangle)^2 \rangle. \tag{3}$$

(1) represents the mean displacement of the electrons in the field direction from which the drift velocity $w = d\langle z \rangle/dt$ can be obtained; the transversal diffusion coefficient and the longitudinal diffusion coefficient arise respectively from (2) and (3) from Fick's equations [1, 6]:

$$D_T = \frac{1}{4} \frac{d}{dt} \langle x^2 + y^2 \rangle \tag{4}$$

and

$$D_L = \frac{1}{2} \frac{d}{dt} \langle (z - \langle z \rangle)^2 \rangle. \tag{5}$$

When the Monte Carlo simulation is used to obtain the drift velocity of the charge carriers at low applied field, the statistical uncertainty originating from the thermal motion may become particularly large especially when the ohmic mobility is sought. For this case, then, it is more convenient to evaluate the diffusion coefficient at very low field (approximately zero field) and then to obtain the ohmic mobility by means of the Einstein relation:

$$\frac{kT}{e} = \frac{D_T}{\mu} \tag{6}$$

where μ and e are the electronic mobility and charge respectively. Such a relation holds in general (both in the classical and quantum case) for a system of non-interacting particles [7] as in our case. We report in figure 1 on the temporal behaviours of $\langle z \rangle$ (curve A) and of $\langle x^2 + y^2 \rangle$ (curve B) for a system in which the Fermi energy is 1 eV, the Debye temperature is 0.1 eV and the lattice temperature is 77 K. It is evident that the curve B reaches stationarity after a very short time; on the contrary it is doubtful whether the drift velocity, represented by the angular coefficient of curve A, reaches a reliable value in the reported times. However, the mobility obtained by the drift velocity and the diffusion coefficient are quite different. According to a commonly accepted point of view [1] the diffusion coefficient is a much more accurate estimator for μ .

The Monte Carlo method for charge transport is based on a semiclassical description in which an electron (or N electrons) is simulated as a classical particle subjected to

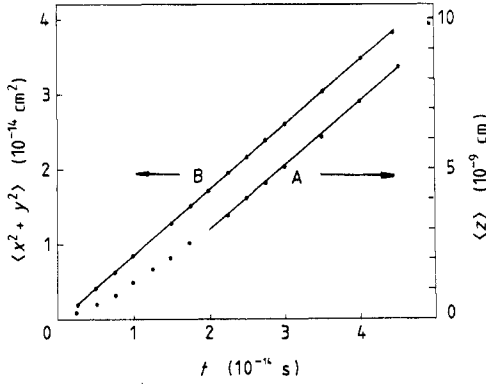


Figure 1. Temporal behaviour of $\langle z \rangle$ (curve A) and $\langle x^2 + y^2 \rangle$ (curve B) obtained by computer simulation of the motion of $\sim 10^5$ electrons in a system in which $\epsilon_F = 1$ eV, $\hbar\omega = 0.1$ eV and $T = 77$ K.

a scattering rate $S(\mathbf{k}, \mathbf{k}')$ obtained by means of perturbation theory. The total scattering rate describing the transition between any two states \mathbf{k} and \mathbf{k}' is given by

$$W(\mathbf{k}, \mathbf{k}') = S(\mathbf{k}, \mathbf{k}') [f(\mathbf{k})(1 - f(\mathbf{k}')) - f(\mathbf{k}')(1 - f(\mathbf{k}))] \quad (7)$$

the two terms in the square brackets corresponding to loss and gain terms as in the scattering integral of the Boltzmann equation. In fact, the Monte Carlo technique is completely equivalent to solving the Boltzmann equation [3]. In the first term of the right hand side of equation (7) \mathbf{k} is the initial state with probability $f(\mathbf{k})$ of being occupied, and \mathbf{k}' is the final state with probability $(1 - f(\mathbf{k}'))$ of being empty, and vice versa for the second term. In the case where the Pauli exclusion principle can be neglected, $f(\mathbf{k}')(f(\mathbf{k})) \simeq 0$ since there is no restriction on the occupancy of the final state. In order to select the final states, $f(\mathbf{k}')$ ($f(\mathbf{k})$) should be considered in (7) but, since it is not known *a priori* and we know only its evolution time during the simulation, we make recourse to an algorithm [5] in which the selection is achieved by means of a self-scattering mechanism with the probability $1 - f(\mathbf{k}')$ or $(1 - f(\mathbf{k}))$. We report a very brief description of the algorithm: a grid in k -space is performed and each cell c contains at maximum $N_c = 2(N/8\pi^3)\Delta\Omega$ electrons, where $\Delta\Omega \simeq 10^{-18}$ cm⁻³ is the volume of the cell c . When an electron is submitted to a scattering event, the cell c relative to the final state is found, then a distribution function f_c for the cell c is defined and normalised to N_c . A rejection technique is used on comparing the normalised f_c with a random number $0 < r < 1$; if $f_c < r$ the electronic transition is allowed and the new final state is accepted, if $r < f_c$ the scattering mechanism is rejected and the electronic wavevector is unchanged. As verified in our previous paper [4] and reported also in the results of this paper, $f(\mathbf{k}', t)$ remains similar to the Fermi function at the temperature of interest; for this reason it is possible to apply the rejection technique directly in the energy space using the Fermi–Dirac distribution modified flight after flight from the dynamic of the simulation, without introducing any grid in the k -space and reducing in this way the computer time needed for the simulation.

By using the golden rule [8] $S(\mathbf{k}, \mathbf{k}')$ can be calculated in the form

$$S(\mathbf{k}, \mathbf{k}') = g^2 \delta(\epsilon_{\mathbf{k}} - \epsilon_{\mathbf{k}'} \mp \hbar\omega) (n(\hbar\omega) + \frac{1}{2} \pm \frac{1}{2}) \quad (8)$$

where $n(\hbar\omega)$ is the Bose function, $\epsilon_{\mathbf{k}}$ and $\epsilon_{\mathbf{k}'}$ are initial and final electron energies, the \pm sign refers to absorption/emission, and the coupling constant is given by [9]

$$g^2 = \frac{V^2 \hbar q_D}{2NMv_s} \quad (9)$$

in which V is the deformation potential, q_D the Debye wavevector, N the total number of ions of mass M , and v_s the velocity of sound. From (8), the differential cross section for the scattering processes can be evaluated [10]. In our Monte Carlo simulation the scattering processes can be considered isotropic if the momentum transfer cross section (weighted with the factor $(1 - \cos \theta)$) is used [11]. In order to evaluate the duration of the electron flight we use a Rees technique [12], as usual, in which the collision frequencies rather than the cross sections are needed.

For our simulations we use a model with a constant frequency ω of an acoustic branch of the order of the Debye frequency, neglecting the wavevector dependence, as frequently done in the self-energy expression for the electron–phonon interaction [13]. The use of a constant coupling g^2 and a q -independent frequency ω permits us to neglect the $\cos \theta$ term which averages to zero. Such an approximation within the Monte Carlo technique is justified as we shall discuss in a next paragraph. This model may be improved without difficulty to account for an $\omega(q)$, but the results obtained from the simpler model turn out to be accurate enough. Some preliminary results considering such a dependence through the inclusion of a limited number of wavevectors (of the order of three or four) show a stabilisation of the results. In this approximation the collision frequencies needed in the Rees technique turns out to be

$$v(\epsilon) = A\sqrt{\epsilon \mp \hbar\omega} (n(\hbar\omega) + \frac{1}{2} \pm \frac{1}{2}) \quad (10)$$

where $A = 2.71 \times 10^{13} V^2 m^{*3/2} q_D / \rho v_s$ in which the density ρ of the crystal is in g cm^{-3} , the sound velocity v_s in 10^5 cm s^{-1} , the Debye wavevector q_D in 10^8 cm^{-3} and the deformation potential V in eV. To obtain equation (10), the density of states is assumed varying with the energy as $\epsilon_k^{1/2}$ for a 3D case. A generalisation of this formula to a generic dimensionality is easily found. Some detailed calculations are in progress for a 2D case motivated by the anisotropy of the resistivity in some materials of actual interest such as ceramic superconductors and will be reported elsewhere. The values of the parameters used in our collision frequencies are reported in table 1.

Table 1. Values of the parameters used in the expression of the coupling constant as in equation (11).

V (eV)	q_D (10^8 cm^{-3})	ρ (g cm^{-3})	v_s (10^5 cm s^{-1})
$\sqrt{10}$	1	1	1

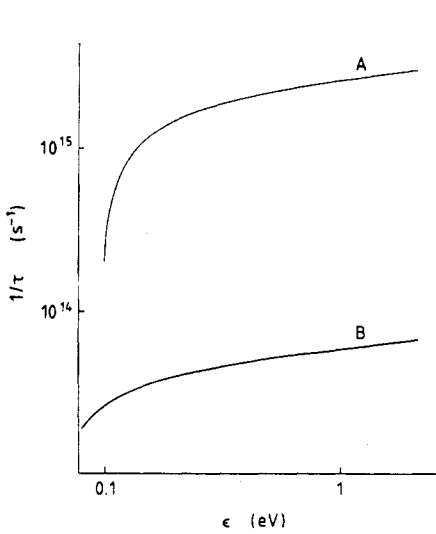
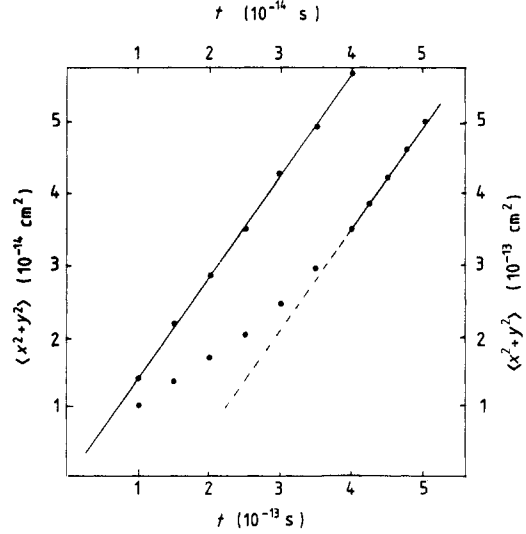
In the literature [8] the expressions for the collision frequencies for electron–phonon coupling in metals are reported neglecting the zero-point term contained in equation (10). The zero-point term is considered in our model because at low temperature its effect is strong thus increasing the emission process as we can see in figure 2 where we have reported the collision frequencies used by us at $T = 30 \text{ K}$ and leading to considerable energy loss around the Fermi level. In table 2 we report the values characterising the different simulated systems with the resistivity values found at room temperature.

3. The results

The results obtained by means of our Monte Carlo simulation for the values of the transport parameters are affected by not too large fluctuations as in previous work [3]

Table 2. Parameters characterising the physical systems studied by computer simulation and obtained values of resistivity at room temperature.

ϵ_F (eV)	θ_D (eV)	m^*/m_0	ρ (Ω cm)	Physical system
1	0.1	1	4.8×10^{-18}	Simple metal
0.1	0.01	1	1.31×10^{-15}	Metal with few carriers
0.1	0.04	5	9.8×10^{-15}	YBaCuO [12]


Figure 2. Electron one-phonon collision frequencies for emission (curve A) and absorption (curve B) used in our Monte Carlo simulation. It should be noted that the emission frequency has a threshold at $\hbar\omega$. Parameters are $\epsilon_F = 1$ eV, $\hbar\omega = 0.1$ eV and $T = 300$ K.

Figure 3. Temporal behaviour of $\langle x^2 + y^2 \rangle$ obtained by the simulation with the initial energy distribution $g(\epsilon, 0) = g(\epsilon, \infty)$ (curve A, upper temporal scale and left length scale) and $g(\epsilon, 0) \neq g(\epsilon, \infty)$ (curve B, lower temporal scale and right length scale). In the second case $g(\epsilon, 0)$ is a flat distribution centred around the Fermi level ($\epsilon = 1$ eV, $\hbar\omega = 0.1$ eV and $T = 300$ K).

and considered as acceptable in work of this kind. They show that we are simulating a metal by comparing the results with the theory of metals [11] in analytic form.

3.1. Stationarity

The times of stationarisation of the simulated system are studied using two different initial energy distributions of electrons: $g(\epsilon, 0) = g(\epsilon, \infty)$ and $g(\epsilon, 0) \neq g(\epsilon, \infty)$. In particular, for the second case, we use a flat distribution centred around the Fermi level. In figure 3 we report the temporal behaviour of the quantity $\langle x^2 + y^2 \rangle$, which is of main interest for us, for the two cases. Although it is difficult to make clear the results because the stationarisation times are very different (almost by two order of magnitude) nevertheless it can be seen that by using $g(\epsilon, 0) = g(\epsilon, \infty)$ the steady state is reached after 10^{-14} s which corresponds to $\simeq 100$ scattering events for each electron, while in the case in which $g(\epsilon, 0) \neq g(\epsilon, \infty)$, approximately 4×10^{-13} s are needed in order to reach a stationary behaviour, greatly increasing the computer time needed. It

should be noted that after reaching stationarity, for both cases the results are equal as can be verified by the slopes of the two curves.

3.2. Ohmicity

Owing to the difficulties quoted before in obtaining reliable values of the drift velocity, we can only test the ohmicity of the system by the transversal diffusion coefficient which remains unchanged on varying the electrical field. The results obtained in this way for four values of the electrical field are reported in table 3 where one can see that as expected the behaviour of the system is ohmic within a percentage error of three.

3.3. Energy distribution functions

In figure 4 we give two energy distribution functions obtained on simulating a system for which the Fermi level is 1 eV and the Debye temperature is 0.1 eV at temperatures $T = 77$ K (curve A) and $T = 300$ K (curve B). As previously stated and expected, the distributions are similar in form to the Fermi–Dirac distribution but distorted by the electron–phonon coupling, the distortion being more pronounced around the Fermi level where the transport processes occur. The broken curve describes the ideal case.

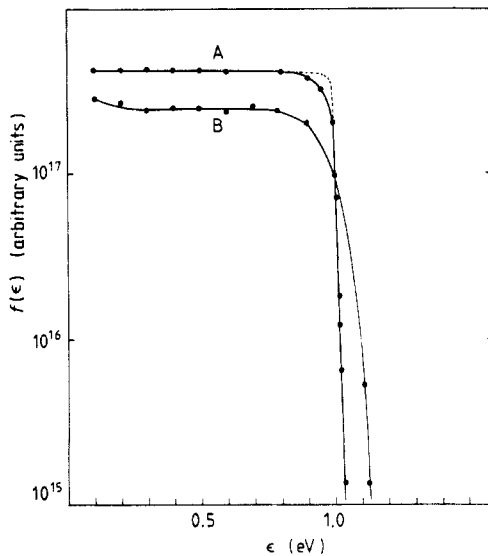


Figure 4. Energy distribution function as obtained in present work. Parameters are $\epsilon_F = 1$ eV, $\hbar\omega = 0.1$ eV and $T = 77$ K (curve A) and $T = 300$ K (curve B). The broken line refers to the ideal case at $T = 77$ K.

3.4. Resistivity versus temperature

The main results of our Monte Carlo simulations concerning the behaviour of the resistivity versus temperature are comparable with the theory of metals, developed by a transport Boltzmann equation [11]. In a system in which $\epsilon_F = 0.1$ eV and $\theta_D \simeq 116$ K, as one example, we have considered two regions of high temperatures $T \gg \theta_D$ and low temperatures $T \ll \theta_D$ where the theory provides two kinds of behaviour:

$$\rho = a \frac{T}{\theta_D^2} \quad \text{for } T \gg \theta_D \quad (11)$$

and

$$\rho = bT^5 \quad \text{for } T \ll \theta_D \tag{12}$$

where $a = 9.9 \times 10^{-19}$ and $b = 2.97 \times 10^{-25}$ with the values of the parameters used in this paper. The strong temperature dependence of the metallic resistivity described by equation (12) is a characteristic quantum effect in a 3D system, obtained by the cut-off of the Bose function at $\omega/kT > 1$ on the collision frequencies and weighted by the $(1 - \cos \theta)$ factor. Our results are reported in figure 5 and 6 for high and low temperatures respectively, and they are in very good agreement with the theory comparing the values obtained for the parameters $a = 1.7 \times 10^{-18}$ and $b = 3.2 \times 10^{-25}$ by the Monte Carlo simulation with the values of equation (11) and (12) obtained by the Boltzmann approach.

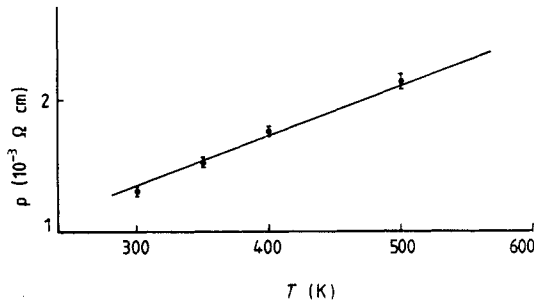


Figure 5. Resistivity versus temperature at $T \gg \theta_D$. The system parameters are: $\epsilon_F = 0.1$ eV, $\theta_D = 116$ K. The angular coefficient of the straight line is $a = 1.7 \times 10^{-18}$.

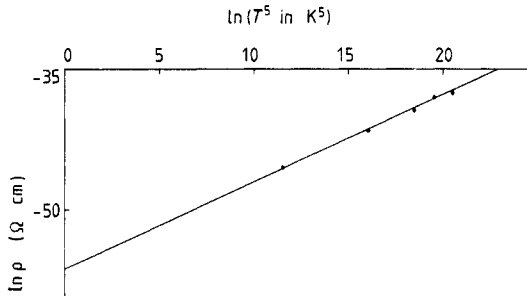


Figure 6. The logarithmic behaviour versus $\ln T^5$ for $T \ll \theta_D$ with the same parameters as in figure 4. The angular coefficient of the straight line is $b = 3.2 \times 10^{-25}$.

One should note that, in the Boltzmann approach, where the emission and absorption processes are not distinguished, the T^5 law arises from the q -dependence of $g^2 (\propto q)$, $\omega (\propto q)$ and $1 - \cos \theta \propto q^2$ as well as the q^2 -dependence of scattering space in 3D [8, 10]. In a rigorous approach [11, 14], in which phonon emission and absorption processes are treated separately, the inclusion of the zero-point term is consistent with the T^5 law. This is the same conclusion as we find by our Monte Carlo simulations.

From table 2 we can also note that the orders of magnitude of the resistivity obtained by Monte Carlo simulation are in agreement with the experimental ones in the different physical systems examined.

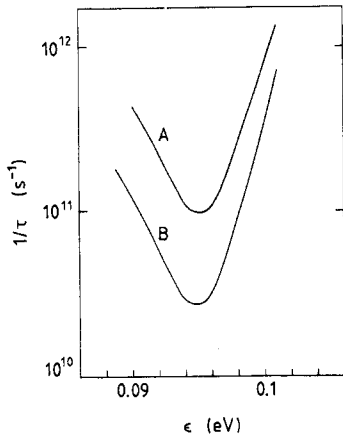


Figure 7. Many-body (including the Fermi functions) total collision frequencies for electron-phonon scattering from the first-order perturbation theory (curve A) and from renormalised electron self-energy (curve B). Parameters are $\epsilon_F = 0.1$ eV and $\hbar\omega = 0.01$ eV at $T = 15$ K.

3.5. Mean energy

Another parameter which can be obtained by means of the simulation is the electron mean energy. Some values obtained in the simulation indicate that they are lower than the known free values $\bar{\epsilon} = \frac{3}{5}\epsilon_F$ especially at low temperatures indicating a dominant emission mechanism as in figure 2. These are given in table 3.

Table 3. Values of transversal diffusion coefficients obtained by Monte Carlo simulation at different electrical fields. The parameters of the system are $\epsilon_F = 0.1$ eV, $\theta_D = 116$ K and $T = 50$ K. In the last column we report the percentage error with respect to the mean value of 1.31×10^{-1} cm² s⁻¹.

E (V cm ⁻¹)	D_T (cm ² s ⁻¹)	Δ
0.1	1.29×10^{-1}	2.08
0.5	1.28×10^{-1}	2.85
1	1.35×10^{-1}	-2.46
1.5	1.35×10^{-1}	-2.46

4. Conclusions

The results presented in this paper suggest that the Monte Carlo technique may be suitable for the study of transport properties of metals, with acceptable statistical fluctuations at the low fields that can be applied to systems in the ohmic regime. They suggest that it may become particularly useful to investigate more realistic situations not accessible by the simple theory of metals once the collisions frequencies are known.

In this respect, one of the possible developments we envisage is the study of renormalisation effects on the transport mechanisms to account for a coupling of electrons with the lattice vibrations strong enough to be outside the possibility of the perturbative description. The renormalisation influences the scattering frequencies, as one can see in figure 7, producing at low temperature a stronger depression around the Fermi level and this fact can be introduced within the Monte Carlo procedure relatively easily. Preliminary results under investigation show that the stronger coupling corresponds to higher resistivity at high temperature, but also to an enhancement of the quantum effects with an increase to the power five in (12).

Another field of investigation which appears promising is the inclusion of various scattering phonon processes, as may arise for example from optical and polar branches or diverse acoustic subbranches of the lattice with more than one ion per unit cell. Such a procedure is already successful in different systems in which the stoichiometric composition is relevant [3, 15] and appears possible also for metals. Finally one may envisage the use of the Monte Carlo technique for the study of conductivity fluctuations close to the superconducting transition, at which the resistivity becomes very small.

Acknowledgment

It is a pleasure to thank Professor P Lugli for valuable assistance and discussions on various aspects of the Monte Carlo technique.

References

- [1] Price P J 1969 *Semiconductors and Semimetals* (New York: Academic) p 249
- [2] Zimmermann J, Lugli P and Ferry D K 1983 *Solid State Electron.* **26** 233
- [3] Jacoboni C and Reggiani L 1983 *Rev. Mod. Phys.* **55** 645
- [4] Romanó L and Dallacasa V 1988 *Vuoto* **18** 202
- [5] Lugli P and Ferry K 1985 *IEEE Trans. Electron Devices* **ED-32** 2431
- [6] Jacoboni C, Gagliani G, Reggiani L and Turci O 1978 *Solid State Electron.* **21** 315
- [7] Kubo R 1957 *J. Phys. Soc. Japan* **12** 6570
- [8] Pines D 1963 *Elementary Excitation in Solids* (New York: Benjamin) p 273
- [9] Ridley B K 1982 *Quantum Processes in Semiconductors* (Oxford: Clarendon) p 126
- [10] Ziman J M 1972 *Principles of the Theory of Solids* (Cambridge: Cambridge University Press) p 221
- [11] Braglia G L 1977 *Physica C* **92** 91
- [12] Rees H D 1968 *Phys. Lett.* **26A** 416; 1969 *J. Phys. Chem. Solids* **30** 643
- [13] Engelsberg S and Schreiffner J R 1963 *Phys. Rev.* **131** 993
- [14] Jones H 1956 *Encyclopedia of Physics* vol 19 (Berlin: Springer)
- [15] Braglia G L, Romanó L and Roznerski W 1984 *Control Plasma Phys.* **24** 113